Novel Multipactor Studies in RF Satellite Payloads: Single-Carrier Digital Modulated Signals and Ferrite Materials

D. González-Iglesias, Ó. Monerris, B. Gimeno, *Member, IEEE*, M. E. Díaz, V. E. Boria, *Senior Member, IEEE*, P. Martín, Á. Gómez, Ó. Fernández, A. Vegas, *Member, IEEE*, F. Casas, S. Anza, C. Vicente, J. Gil, R. Mata, I. Montero, D. Raboso

***Abstract*—In this work it is reviewed the most novel advances in the multipactor RF breakdown risk assessment devoted to RF satellite microwave passive devices employed in space telecommunication systems. On one side, it is studied the effect of transmitting a single-carrier digital modulated signal in the multipactor RF voltage threshold in a coaxial line. On the other hand, an analysis of the multipactor phenomenon in a parallel-plate waveguide containing a magnetized ferrite slab it is presented.**

***Index Terms*—Multipactor, digital modulations, ferrite materials.**

I. Introduction

Multipactor breakdown is an high RF power phenomenon that takes presence in vacuum environments when there is a synchronism between the RF electric field and the free electrons within the device [1]. Under certain conditions, electrons impacting with the component walls are able to release one or more secondary electrons from the surface, thus starting a resonant chain that leads to an exponential increase of the electron population within the device. When the electron number is very high it appears an electric current between the walls of the component that has several negative effects that degrade the performance, such as increasing the signal noise and reflected power, heating up the device walls, outgassing, detuning of resonant cavities, and even resulting in the total destruction of the component. The multipactor discharge is present in many different environments such as passive components of satellite communication payloads, particle accelerators, and klystrons.

Focusing on telecommunication systems, special attention must be paid to multipactor in satellite components, where replacement of damaged devices is not possible. Therefore, in order to ensure that the RF component will not suffer this undesirable phenomenon during operation, it is extremely important to take into account this effect in the design process.

This paper presents a short summary of some recent multipactor studies focusing on two different topics: the analysis of the multipactor effect in a coaxial transmission line excited with a single-carrier digital modulated signal, and the multipactor phenomenon in a parallel-plate waveguide partially filled with a magnetized ferrite slab. In the next section, it is described the theoretical frame in which is based the in-house developed software for the multipactor numerical simulations. Then, the most remarkable results of the aforementioned cases are shown. Finally, the most relevant conclusions of both studies are outlined.

II. Theory

A Monte-Carlo software to analyze the multipactor effect in microwave components has been developed. This algorithm combines the advantages of the individual electron and effective electron models. At the beginning of the multipactor simulation, individual electrons are considered; if during the simulation the electron population exceeds a certain threshold, then the individual electrons switch into effective ones. From then on, these effective electrons start to accumulate charge and mass instead of generating new particles. In this way, the computational cost remains constant.

For each tracked particle, the 3-D trajectory is computed by solving the non-relativistic differential equation of motion using the Velocity-Verlet algorithm. The differential equation of motion that governs the electron dynamics is derived from the Lorentz Force, which depends on the total electric and magnetic fields that experiences the electron. The total electromagnetic field is the superposition of the RF electromagnetic field and the electric field due to the space charge effect that takes into account the Coulomb repulsion among the electrons. For the coaxial transmission line, the RF electromagnetic field is the correspondent to the fundamental coaxial TEM mode

D. González-Iglesias and Ó. Monerris are with the Val Space Consortium, Valencia, Spain, (email: daniel.gonzalez-iglesias@uv.es; oscar.monerris@val-space.com)

B. Gimeno and R. Mata are with Depto. Física Aplicada-ICMUV, Universidad de Valencia, Spain (email: benito.gimeno@uv.es; rafael.mata@uv.es)

M. E. Díaz is with Depto. de Informática, ETSE, Universidad de Valencia, Spain, (email: elena.diaz@uv.es)

V. E. Boria is with Depto. Comunicaciones-iTEAM, Universidad Politécnica de Valencia, Spain (email: vboria@dcom.upv.es)

P. Martín and D. Raboso are with European Space Agency, ESA/ESTEC, The Netherlands (email: petronilo.martin.iglesias@esa.int, david.raboso@esa.int)

Á. Gómez, Ó. Fernández, and A. Vegas are with Depto. Ingeniería de Comunicaciones, Universidad de Cantabria, Spain (email: alvaro.gomez@unican.es; oscar.fernandez@unican.es; angel.vegas@unican.es)

F. Casas is with Instituto Universitario de Matemáticas y Aplicaciones (IMAC), Universidad Jaume I, Castellón, Spain (email: casas@uji.es)

S. Anza, C. Vicente and J. Gil are with AURORASAT, Valencia, Spain (email: sergio.anza@aurorasat.es; carlos.vicente@aurorasat.es; jordi.gil@aurorasat.es)

I. Montero is with Instituto de Ciencia de Materiales de Madrid, CSIC, Madrid, Spain (email: imontero@icmm.csic.es)

carrying the digitally modulated signal. For the parallel-plate waveguide loaded with the ferrite slab, the RF electromagnetic field is those corresponding to the fundamental propagative mode, which has been obtained with the aid of the Coupled Mode Method (CMM) [2]. Besides, in the ferrite case, there are an external static magnetic field which is the responsible of the anisotropic behavior of the ferrite, and a static electric field that arises from the dielectric polarization of the ferrite slab when it absorbs or emits electrons. Both the electric space charge and polarization fields are computed following the procedure reported in [3].

At each integration step, the code checks if the electron collides with any of the waveguide walls. The interactions of electrons with surfaces are considered by means of the Secondary Electron Yield (SEY) function. In this work, we have been implemented such contributions according to the Furman and Pivi formulas described in [4] in the case of the digital modulations in the coaxial line. On the other hand, a modification of the Vaughan's model presented in [5] is preferred for the ferrite waveguide case. After the collision, the true secondary electrons depart from the impact point with a random velocity following a Maxwellian distribution with a mean average energy of 3 eV and an elevation angle that follows the Cosine Law [6].

III. Results

A. Digital modulated signal in a coaxial transmission line

This subsection presents the multipactor RF voltage threshold results for the coaxial transmission line excited with the single-carrier digital modulated signal. The dimensions of the coaxial line used throughout this work are: $a = 1.238$ mm and $b = 2.850$ mm, thus the gap length is $d = b - a = 1.612$ mm; the coaxial characteristic impedance is $50\,\Omega$. Both conductors are made of copper. According to the model proposed in [4], the fitting parameters for the true secondaries SEY contribution are: $\delta_m = 1.77$, $W_m = 277$ eV, and $s = 1.539$. For all considered modulation schemes, the RF carrier frequency is $f = 1.145$ GHz, and the signal is filtered with a root-raised-cosine filter with a roll-off factor of 0.2.

In addition to the results obtained from multipactor numerical simulations, a coarse method based on the envelope integration for a roughly estimation of the RF multipactor voltage threshold with an arbitrary digitally modulated signal was also employed. This method exclusively uses the results obtained from numerical simulations with a non-modulated single carrier signal, presenting the advantage of being much faster than individual electron numerical simulations for the digitally modulated signals.

In order to consider realistic signals, a random symbol sequence has been generated for each of the following digital modulations: Quadrature Phase-Shift Keying (QPSK), 16Amplitude and Phase-Shift Keying (16APSK), 32Amplitude and Phase-Shift Keying (32APSK), and 16Quadrature (16QAM)[1]. Besides the symbol sequence, the other modulation parameter that most influences the multipactor phenomenon is the ξ factor, which is defined as the ratio between the symbol duration T_s and the RF carrier period $T = 1/f$, i.e., $\xi = \frac{T_s}{T}$.

[1]Telecom signals of ESA Galileo constellation provided by ESA contract no. 4000111147/14/NL/GLC.

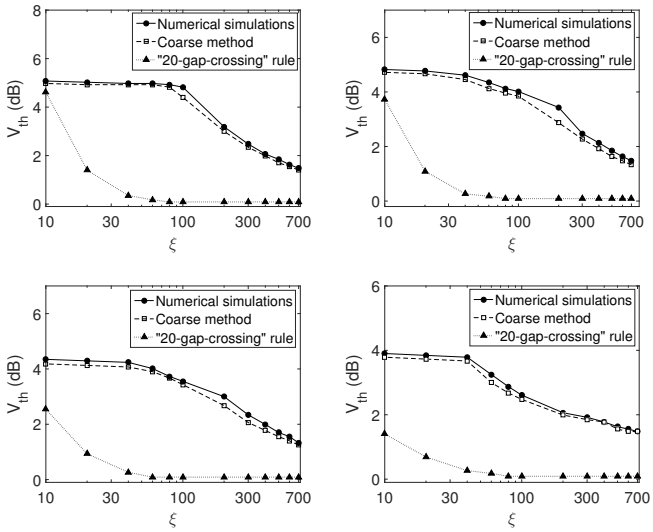

Fig. 1. RF multipactor voltage threshold in dB as a function of the ξ factor for the random symbol sequences. From left to right and up to down: QPSK, 16APSK, 32APSK, and 16QAM. Results for the numerical simulations, the coarse method, and the "20-gap-crossing" rule are shown.

The RF multipactor voltage threshold in dB for each of the transmitted signals, as a function of the ξ factor, is shown in Fig. 1. The RF multipactor voltage threshold of a digitally modulated signal, expressed in dB, is defined taking as $V_{th}(dB) = 20\log(V_{th}/V_{th,CW})$, $V_{th,CW}$ being the multipactor RF voltage threshold for the CW signal at the carrier frequency. The theoretical results provided by the numerical simulations and the coarse method are also compared with the "20-gap-crossing" rule used in the space standard document ECSS-E20-1A.

An experimental test campaign to validate the theoretical results was performed at the ESA-VSC European High Power RF laboratory [7]; the experimental setup is similar to the standard one for multipactor measurements described in [8]. The data obtained from the multipactor measurements have been summarized in Fig. 2, where the theoretical results are also included. On the one hand, it is observed good concordance between the experimental results and the numerical simulations, demonstrating the feasibility of the developed code to predict the RF multipactor voltage threshold with digitally modulated signals. In addition, it is found acceptable agreement of the experimental data with the coarse method. On the other hand, it is noticed the remarkable discrepancies found between the results of the experiment and the predictions provided by the "20-gap-crossing" rule.

B. Parallel-plate waveguide with a magnetized ferrite slab

In this subsection it is presented the study of the multipactor effect in an ideal uniform parallel-plate waveguide of infinite length along the x and z axis, z being the propagation direction of the electromagnetic wave, thus resulting an electromagnetic field which does not depend on the x-coordinate. The waveguide contains a lossless ferrite slab which is magnetized

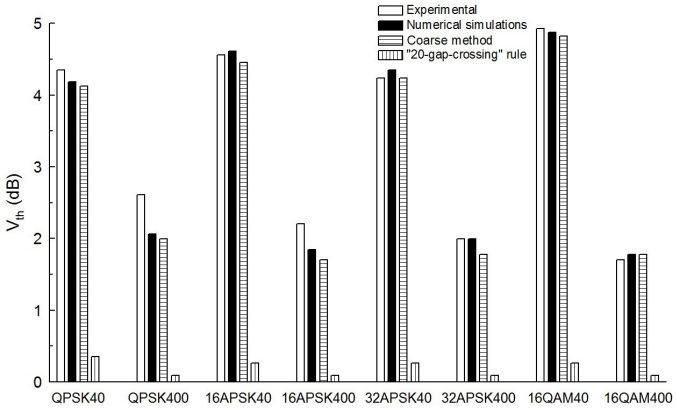

Fig. 2. RF multipactor voltage threshold in dB for different digital modulated signals. In both cases the number after the modulation name indicates the ξ value.

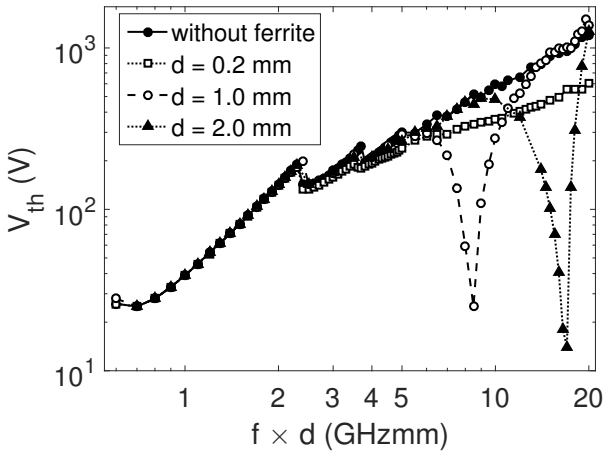

Fig. 3. Multipactor RF voltage threshold as a function of the frequency gap for the parallel-plate ferrite loaded waveguides with different gap lengths and ferrite thicknesses (but maintaining the height of a WR-90 waveguide); and also for a metallic parallel-plate waveguide ("without ferrite").

along the direction perpendicular to the metallic walls. The anisotropic magnetic permeability of the ferrite is given by the Polder's tensor (eq. 9.27 of [9]).

In order to compute the multipactor RF voltage threshold for the parallel-plate ferrite loaded waveguide numerical simulations have been performed. In all cases, the ferrite thickness h and the vacuum gap d have been selected to match with the height of a WR-90 rectangular waveguide, i.e. $b = d + h = 10.16$ mm. The saturation magnetization of the ferrite is $4\pi M_s = 1806$ G, its relative dielectric permittivity $\varepsilon_r = 15$, and its SEY parameters according the modified Vaughan's model [5] are: $W_1 = 19$ eV, $\delta_{max} = 2.88$, and $W_{max} = 289$ eV. For simplicity, the same SEY parameters are selected for the top metallic wall. The external magnetic field employed to magnetize the ferrite is $H_0 = 3000$ Oe. The considered fields are those corresponding to the fundamental mode of the ferrite loaded waveguide.

In Fig. 3 the variation of the multipactor RF voltage threshold as a function of the frequency gap value is shown for several ferrite loaded parallel-plate waveguides. Note that for each curve the gap remains fixed. Moreover, the results for a classical metallic parallel-plate waveguide with no ferrite slab, a gap of $d = 0.2$ mm and $H_0 = 0$ (henceforth referred as without ferrite case) has been included for comparison purpose. From the results it is noticed that there is considerable difference between the multipactor RF voltage threshold of the ferrite loaded waveguides and the corresponding to the without ferrite case. It is found that this discrepancy increases with the gap value. In fact, the maximum difference in the multipactor RF voltage threshold between the $d = 0.2$ mm waveguide and the without ferrite case is of 6.5 dB, whilst in the $d = 1$ mm and $d = 2$ mm the difference becomes of 26 dB and 37 dB, respectively. It is also observed that the multipactor behavior of the ferrite loaded waveguides remains very close to the without ferrite case for low frequency gap values (below 2.5 GHzmm). In general terms, the multipactor RF voltage threshold of the ferrite loaded waveguide cases tends to be equal or below the without ferrite multipactor threshold.

IV. Conclusions

In this article it is presented a short summary of the most recent advances in the multipactor RF breakdown studies devoted to an accurate assessment of the discharge risk in RF passive components. Particularly, two different cases are examined. The first one it is related with the transmission of single-carrier digital modulated signals in coaxial lines. An in-house simulation code has been developed for such purpose, finding good agreement when comparing these results with experimental tests. The second topic is related to the multipactor effect in devices containing magnetized ferrites. The particular case of a parallel-plate waveguide containing a ferrite slab magnetized along the gap direction has been analyzed by means of multipactor simulations. The theoretical results predicts noticeable variations in the multipactor RF voltage threshold with regard to the case without ferrite.

References

[1] J. Vaughan, "Multipactor", *IEEE Trans. Electron Devices*, Vol. 35, No. 7, pp. 1172-1180, July 1988.

[2] S.A Schelkunoff, "Generalized telegraphist's equations for waveguides", *Bell Syst. Tech. J.*, vol. 3, no. 4, pp. 784-801, July 1952.

[3] A. Coves, G. Torregrosa-Penalva, C. Vicente, B. Gimeno, and V. E. Boria, "Multipactor discharges in parallel-plate dielectric-loaded waveguides including space-charge effects", *IEEE Trans. on Electron Devices* vol. 55, no. 9, pp. 2505-2511, Sep. 2008.

[4] M. A. Furman and M. T. F. Pivi, "Simulation of secondary electron emission based on a phenomenological probabilistic model", Lawrence Berkeley Nat. Lab., Univ. California, Berkeley, CA, USA, Tech. Rep. LBNL-52807, Jun. 2003.

[5] C. Vicente, M. Mattes, D. Wolk, B. Mottet, H.L. Hartnagel, J.R. Mosig and D. Raboso, "Multipactor breakdown prediction in rectangular waveguide based components", *Microwave Symposium Digest, 2005 IEEE MTT-S International*, 12-17 June 2005.

[6] J. Greenwood, "The correct and incorrect generation of a cosine distribution of scattered particles for Monte-Carlo modelling of vacuum systems", *Vacuum,* vol. 67, no. 2, pp. 217-222, Sep. 2002.

[7] European Space Agency RF High-Power Laboratory, Valencia, Spain. *Val Space Consortium*. [Online]. Available: http://www.val-space.com

[8] "Multipaction Design and Test", ECSS-E-20-01A, ESA-ESTEC, 2003.

[9] David M. Pozar, "Microwave Engineering", 4th edition, *John Wiley & Sons, Inc.*, 2012.